*Mausam*, (1996), 47, 1, 21-30

551.461.2 : 551.553.21 (267)

# Upper ocean responses in the central western equatorial Indian Ocean during southwest monsoon season

M. G. JOSEPH, P. V. HAREESH KUMAR and P. MADHUSOODANAN
*Naval Physical and Oceanographic Laboratory Thrikkakara, Cochin*
*(Received 19 October 1994, Modified 21 April 1995)*

**सार** — भारत-सोवियत मानसून प्रयोग, 1973 (इसमेक्स-73) के दौरान क्रम से एकत्रित किए गए आंकड़ों का उपयोग करते हुए, हिन्द महासागर में दक्षिण-पश्चिमी मानसून के 0° उत्तर तथा 60° पूर्व की ओर दक्षिण-पश्चिमी मानसून के आरम्भ होने से पूर्व, आरम्भ के समय तथा सक्रिय अवस्थाओं में महासागर के ऊपरी क्षेत्र (200 मी०) पर इसकी प्रतिक्रिया का विश्लेषण किया गया। महासागरीय प्रतिक्रिया के रूप में मानसून के आरम्भ होने से पहले वायु प्रतिबलन के संवेग के प्रभाव का तथा वर्षा ऋतु के दौरान मानसून की सम्मिलित परतों के अन्तर्विस्तार में (एम० एल० डी०) संघनन/ऊष्णन और गहराने/शीतल होने का (चार दिनों में 12 मी०/0.5 सें०) पता चला है। निचली परत में मानसून के आरम्भ होने से पूर्व थर्मोहैलाइन/घनत्व प्रवणता में वृद्धि तथा वर्षा ऋतु के दौरान इसमें ह्रास और उपसतही अधिकतम लवणता (एस० एस० एम०) के लुप्त होने का पता चला है। इस प्रकार से, एम० एल० डी० तथा उसकी अन्तर्निहित ऊष्मा (एच० सी० एम० एल० डी०) के साथ बी० ओ० तथा क्यू० एन० के अधिक सहसंबंध पाए गए हैं। प्रारम्भ तथा अन्त के मिश्रित संवहनी प्रभाव को छोड़कर पवन प्रतिबल द्वारा विघटित गतिक ऊर्जा के उत्पन्न होने के प्रभावी क्षेत्र के अन्तर्गत महासागर के ऊपरी क्षेत्र की प्रतिक्रिया एम० एल० डी० के गहराने/शीतल होने (6 दिनों में 20 मी०/1° सें०) को व्यक्त करती है। निचली परतों के मध्य में थर्मोहैलाइन/घनत्व प्रवणता में परिवर्तन होने तथा एस० एस० एम० की अनुपस्थिति के कारण सक्रिय अवस्था के दौरान अभिवाह फलक्स में वृद्धि होने से एम० एल० डी०, बी० ओ०, पवन प्रतिबल, क्यू० एन० तथा एच० सी० एम० एल० डी० के बीच सहसंबंध महत्वहीन हो जाते हैं। मिश्रित परत प्राचलों के एकल अक्षीय प्रतिरूपण में पर्याप्त एकरूपता पाई गई है।

**ABSTRACT.** Upper ocean (200 m) response under the pre-onset, onset and active regimes of southwest (SW) monsoonal forcing at 0°N, 60°E in the Indian Ocean was analysed, utilising time series data collected during Indo-Soviet Monsoon Experiment, 1973 (ISMEX-73). Oceanic response under the pre-onset domination of the wind stress momentum and onset domination of buoyancy flux ($B_0$) was apparent in shoaling/warming and deepening/cooling (12 m/0.5°C in 4 days) of Mixed Layer Depth (MLD). The pre-onset increase was followed by an onset decrease in below layer thermohaline/density gradient and disappearance of Subsurface Salinity Maximum (SSM). Correspondingly, MLD and its heat content ($HC_{MLD}$) were more correlated to $B_0$ and $Q_N$. Upper ocean response during active regime manifested in deepening/cooling (20 m/1°C in 6 days) of MLD under dominant production of turbulent kinetic energy by wind stress except for the convectively dominant mixing at the beginning and end. With reduction in below-layer thermohaline/density gradient and absence of SSM, the correlations between MLD, $B_0$, wind stress, $Q_N$ and $HC_{MLD}$ became insignificant due to increased advective flux during active regime. One dimensional simulation of mixed layer parameters showed reasonable agreement.

**Key words** — Indian Ocean, Southwest monsoon, Wind stress, Heat flux, Mixed layer, Heat content, Correlations, Simulation.

## 1. Introduction

In the north Indian Ocean, monsoonal influences are dominant in imparting significant changes in the thermohaline/density and current fields of the upper ocean. Consequently, the upper ocean variability differs with the intensity and extent of the forcings by the southwest and northeast monsoons in different areas. However, in the western north Indian Ocean and the Arabian Sea, southwest (SW) monsoon plays the prominent role in the transfer of mass, momentum and heat through the air-sea interface. This, in turn effects the drastic changes in the upper ocean thermohaline and advective fields during May-September, as has been observed earlier. Studies on climatological scales (Mc Phaden 1982, Molinari *et al.* 1986, Shetye 1986, Rao *et al.* 1989) suggested 50 to 75% correlations between the surface mixed layer characteristics and the vertical fluxes of energy and mass through the naviface in western Indian Ocean, north of equator. Some of these also indicated that the correlations increased by including lateral fluxes due to advection and effects of entrainment and wind stress convergence/divergence. Synoptic scale verification of these arguments for the Arabian Sea and western equatorial Indian Ocean during southwest monsoon have been made by means of one dimensional simulations, using time series data sets from MONSOON-77 and MONEX-79, achieving various degrees of agreements and disagreements (Rao 1986, Rao *et al.* 1990, Joseph *et al.* 1990, Sanil Kumar *et al.* 1991). However, presence of significant zonal variability in the

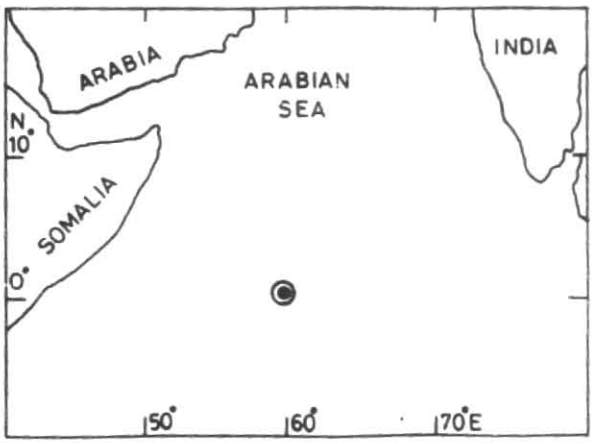


Fig. 1. Station position map for the observations

distribution of monsoonal activity between the East African coast and 75°E (Pant 1976) implies distinct transition zones for vertical fluxes of mass, momentum and heat with varying upper ocean responses along the equator itself. While upper ocean responses in the equatorial regions, west of 50°E are dominated by the cold water advection, vertical fluxes alone are more decisive, east of the reference. In this paper, an effort is made to verify this contention by assessing the synoptic variability in surface forcing by momentum and buoyancy fluxes at 0°N, 60°E. The resulting responses of the thermohaline/density fields in the upper 200 m during the pre-onset and active phases of southwest monsoon and the correlations between forcing parameters and Mixed Layer (ML) characteristics are analysed. Next, the progression of the upper layer parameters are simulated using one-dimensional model and verified with the observed features.

## 2. Data and methods

Processed meteorological and hydrographic data of time series (3 hourly) measurements made on board R. V. Okean during Indo-Soviet Monsoon Experiment, 1973 (ISMEX-73) (Phase I, 27 May-4 June 1973 and Phase II, 25 June-2 July 1973), supplied by India Meteorological Department have been utilised to analyse the air-sea interaction and the upper ocean (200 m) responses at 0°N, 60°E (Fig. 1) in the equatorial Indian Ocean for the pre-onset, onset and active conditions of southwest monsoon. These conditions have been interpretted with regard to *in situ* monsoon conditions over the ship's location and thus, do not refer to the monsoon conditions over mainland India. As no measured solar radiation data is available during the observations, the surface fluxes of net short wave ($Q_i$) and net long wave ($Q_b$) radiations and turbulent fluxes of latent ($Q_e$) and sensible ($Q_h$) heat were estimated, following standard procedures (Lumb 1964, Reed 1976, Atwater and Ball 1981, Payne 1976, Wyrtki 1966, Friehe and Schmitt 1976). The resulting net heat flux ($Q_N$) at the surface was derived using the relationship, $Q_N = Q_i + Q_b + Q_e + Q_h$ with all upward fluxes treated positive and downward fluxes negative. Estimation of MLD of the ocean was based on the oceanic temperature data and was fixed as the shallowest depth where a drop of 0.2°C from sea surface temperature (SST) occurred. Wind stress energy ($E_W$) was estimated using the relationship, $E_W = \tau U$ where, $\tau$, the wind stress $= C_D \rho U^2$. $U$ and $\rho$ are the wind speed and air density respectively. Buoyancy flux ($B_0$) was accounted by means of the surface density changes due to net heating and salinity changes. The relative dominances in forcings by $E_W$ and $B_0$ to surface ML responses were examined by means of Monin-Obukov Length ($L$) and surface mixed layer stability ratio ($D/L$, where, $D$ = MLD). For details of these estimates, Shay and Gregg (1986) and Joseph *et al.* (1992) are referred. For the determination of MLD, isoline depths of temperature, salinity and density (Sigma-T), three point Lagrangian interpolations were made between the standard depth values in the processed data. Heat Content (HC) estimate was made using relationship, $HC = \rho_W C_P \int T\,dz$ where $\rho_W$ and $C_P$ are average density and specific heat at constant pressure of sea water and $T$ is the temperature of the water column of depth element $dz$. On cause-effect basis, MLD is related to wind speed ($U$) and frictional velocity [$U_* = (\tau/\rho_W)^{1/2}$], mixing being proportional to $U^3$ (Turner 1969) or $U_*^3$ (Kato and Phillips 1969) initially and to $B_0$ during deep convections (Shay and Gregg 1986). Linear correlations between MLD, $U^3$ and $U_*^3$ and between $Q_N$ and HC were examined by finding correlation coefficient $r$ and subjecting the same to Student's t-test for significance (Goodwin and Kemp 1979). For simulation of progression of the Mixed Layer Temperature (MLT) and depth (MLD) in response to the wind stress and buoyancy flux, one-dimensional model, following the formulations of Denman (1973) and Miller (1976), was used.

## 3. Results and discussion

### 3.1. *Temporal variability of surface meteorological conditions*

During phase I [Figs. 2 (a & c)], the predominant southwesterly wind was moderate (3 to 10 $ms^{-1}$),

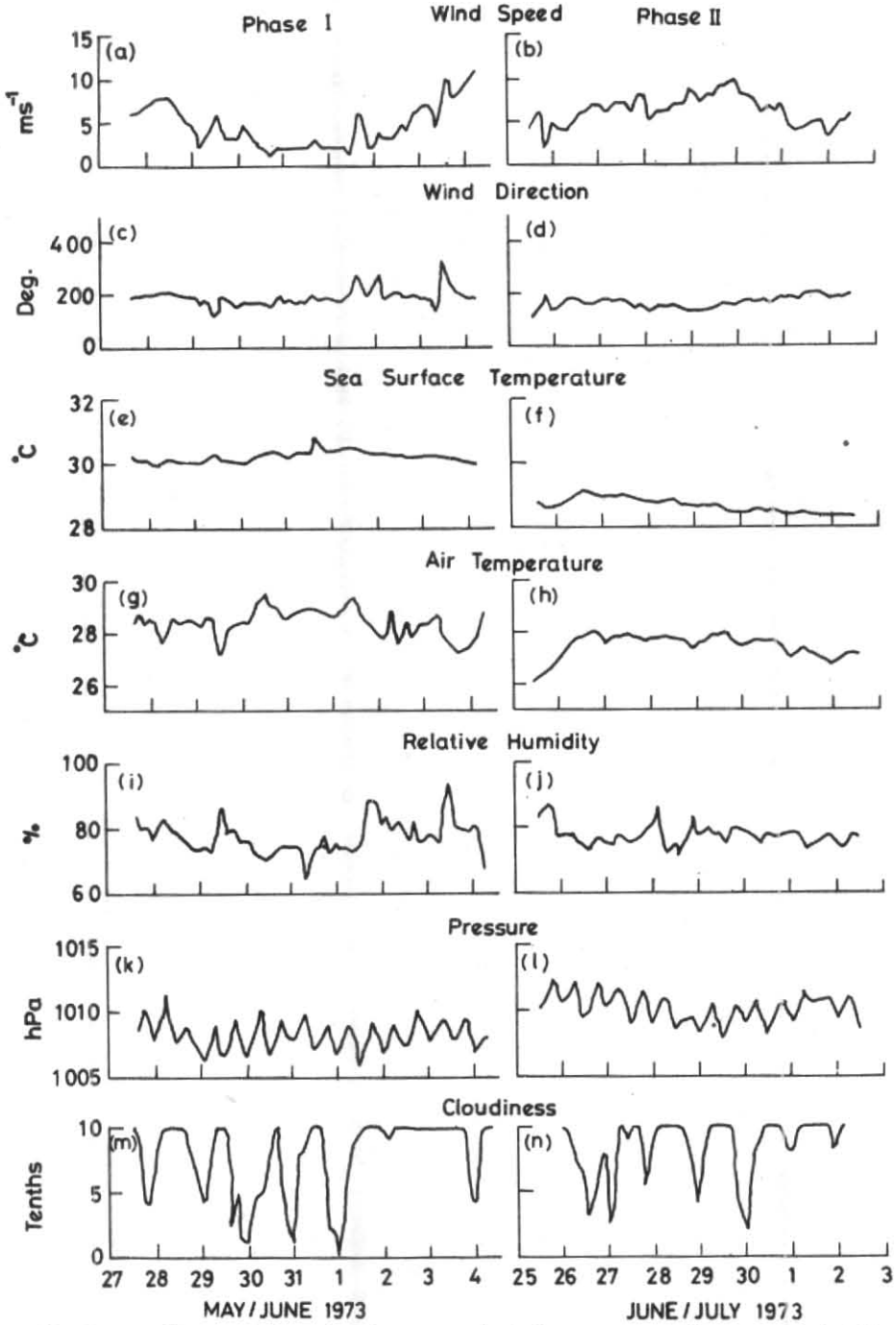


Figs. 2 (a-n). Time variation of surface meteorological parameters during phases I and II

gradually decreasing from 28 to 31 May and suddenly increasing afterwards. Fluctuations in SST (30.0-30.8°C) [Fig. 2 (e)] were superimposed by the diurnal/intradiurnal oscillations with a small drop in magnitude during 31 May-4 June corresponding to the wind increase. Variations in air temperature (AT) (around 29°C) [Fig. 2 (g)] were similar with a drop after 1 June. Changes in relative humidity (RH) (62-90%) [Fig. 2 (i)] were more related to air-sea temperature differences than to wind speeds during this phase. No special influence by any moving system was apparent in the variation of the sea surface pressure (1006 to 1010 hPa) [Fig. 2 (k)] other than diurnal oscillations. The fractional cloud cover (0.2 to 1) [Fig. 2 (m)] varied with an increase after 31 May, becoming mostly overcast thereafter.

The observations during Phase II [Figs. 2 (b & d)], the established phase of the monsoon, indicated the prevalence of southwesterly winds, increasing steadily in strength (5 to 10 $ms^{-1}$) upto 30 June, followed by a decrease. Both SST and AT indicated

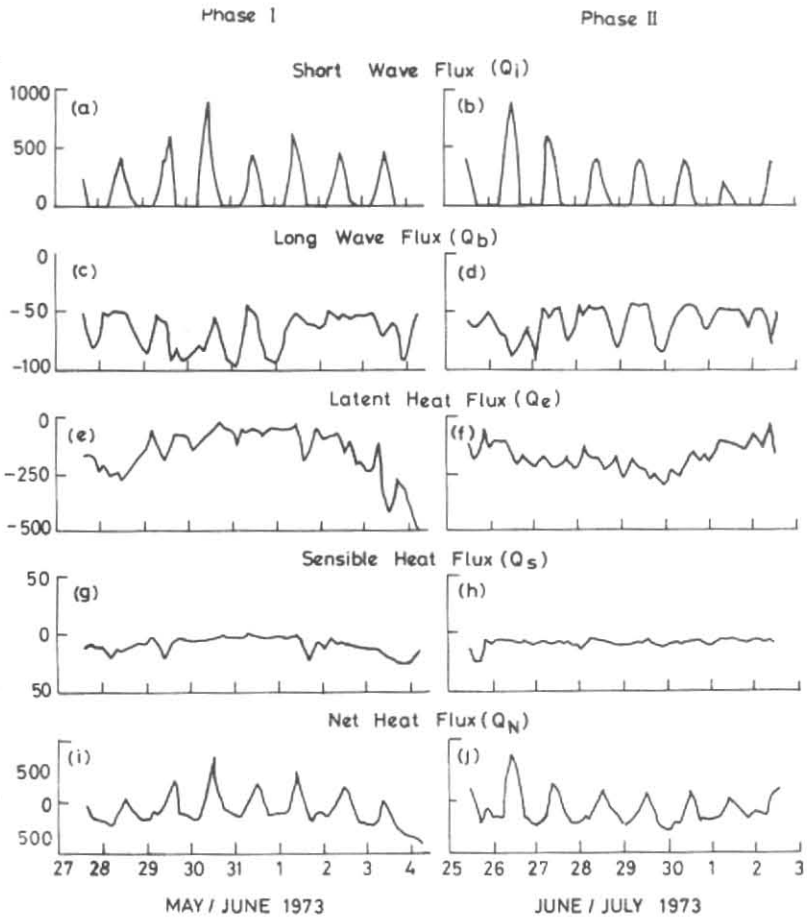


Figs. 3 (a-j). Time variation of the surface heat fluxes during phases I and II

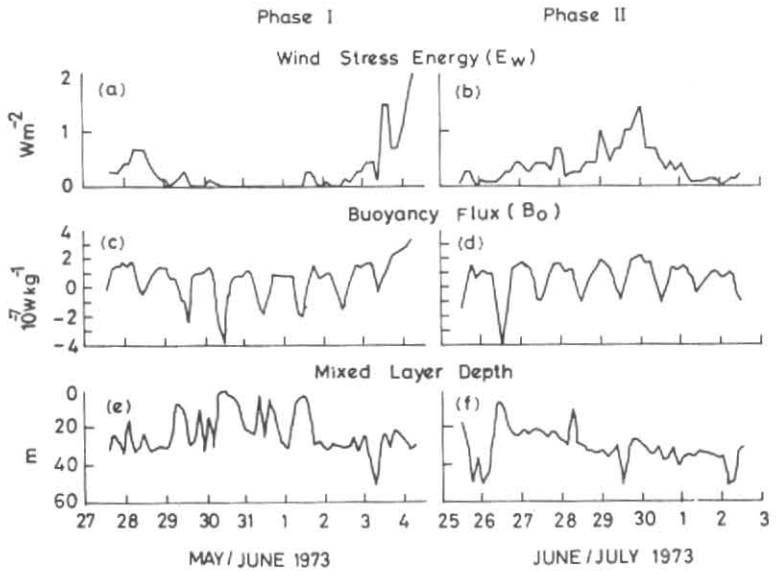


Figs. 4 (a-f). Time variation of wind stress energy ($E_w$), buoyancy flux ($B_0$) at the sea surface and MLD during phases I and II

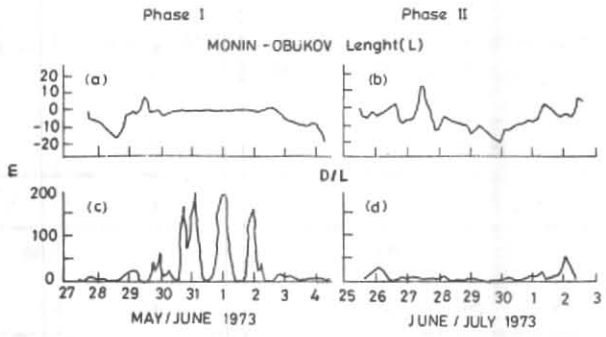


Figs. 5 (a-d). Time variation of Monin-Obukov length ($L$) ad mixed layer stability ratio ($D/L$) during phases I and II

an initial rise on 25 June, followed by a fall (29.1 to 28.4°C and 28 to 27°C respectively) [Figs. 2 (f & h)]. A steady decrease in RH (85 to 70%) [Fig. 2 (j)] after 28 June was indicative of the progressive depletion of the near surface water vapour in the air mass towards the end of the established phase. While a gradual drop in the sea surface pressure [Fig. 2 (l)] from 25 to 28 June was followed by a rise thereafter, fractional cloud cover (0.2 to 1.0) [Fig. 2 (n)] fluctuated during the period.

### 3.2. *Radiative and turbulent heat transfers at the sea surface*

During phase I, the magnitudes of diurnal maxima in the net short wave flux [Fig. 3 (a)] at the sea surface ($Q_i$) (400 to 800 $Wm^{-2}$) depended mainly on the cloudiness as the case of the highest value on 30 May with near-zero cloudiness. The variability in the long wave flux ($Q_b$) (−50 to −95 $Wm^{-2}$) [Fig. 3 (c)] was mainly in response to variations in SST and cloudiness. Changes in the latent heat ($Q_e$) (−30 to −500 $Wm^{-2}$) [Fig. 3 (e)] were pronounced with a gradual decrease from 28 May to 1 June and following sharp rise. The sensible heat ($Q_h$) (−2 to −25 $Wm^{-2}$) [Fig. 3 (g)] flux followed a similar trend with a diminished range. These changes apparently reflected the prominent influences by hikes in wind speed, especially after 1 June. As a result, variations in the net heat flux ($Q_N$) [Fig. 3 (i)] at the sea surface showed the day heating (10 to 650 $Wm^{-2}$) to be increasing to the highest on 30 May and decreasing thereafter. Correspondingly, the diurnal cooling (−15 to −575 $Wm^{-2}$) also increased after 1 June. Decreasing diurnal maxima of $Q_i$ (930 to 225 $Wm^{-2}$) [Fig. 3 (b)] from 25 June to the end of observations could be attributed to the increasing cloudiness during phase II. Variability in $Q_b$ (−45 to −90 $Wm^{-2}$) [Fig. 3 (d)] was with significant diurnal fluctuations. The progressive changes in $Q_e$ (−50 to −300 $Wm^{-2}$) [Fig. 3 (f)] and $Q_h$ (−4 to −25 $Wm^{-2}$) [Fig. 3 (h)] generally reflected the dominant influence by the wind speed and the vapour pressure gradient, resulting in a steady increase of the values upto 29 June followed by a decrease during the established phase of monsoon. A gradual reduction in the diurnal range in $Q_N$ [Fig. 3 (j)] was apparent in this phase, as a result of the progressively decreasing day heating (2 to 680 $Wm^{-2}$) and the nearly steady nocturnal cooling (−20 to −400 $Wm^{-2}$).

### 3.3. *Surface energy fluxes across the air-sea interface and mixed layer responses*

Changes in the TKE production acting to increase the potential energy of ML is proportional to the momentum flux, represented by the wind stress energy ($E_W$). During phase I, variations in $E_W$ (0.07 to 2 $Wm^{-2}$) [Fig. 4 (a)] showed a minimum during 30 May-1 June, after which the wind production increased to maximum. The nocturnal peaks in upward flux of $B_0$ (cooling) (1 to 3.5 × $10^{-7}$W $kg^{-1}$) [Fig. 4 (c)] remained nearly steady upto 1 June and increased thereafter. On the other hand, magnitude of the diurnal peaks in downward fluxes of $B_0$ (heating) (0 to −4 × $10^{-7}$W $kg^{-1}$) changed with a long period (2-3 days) oscillation, increasing to maximum on 30 May under relatively intense heating at less cloudiness and steadily decreasing thereafter. Variability of MLD (−2 to −51 m) [Fig. 4 (e)] reflected the prominent effect of heating ($B_0 < 0$) with the shallowest layer occurring during 30 May-31 June, at the lowest wind stress. On diurnal averages, the pre-onset ML shoaling/warming by12 m/0.5°C in 4 days (27 to 30 May) was followed by the deepening/cooling at the same rate from 31 May to 4 June.

During phase I, convective mixing was active ($L < 0$) in conjunction with wind stress, only during 27-30 May and after 2 June [Fig. 5 (a)]. The changes in $D/L$, indicative of relative dominance for mixing [Fig. 5 (c)] suggest wind stress production to be prominent or equal to buoyancy production ($D/L \leqslant 1$) upto 29/30 May and after 2 June. Increasing convective dominance ($D/L > 1$) existed during the intervening period.

The gradual build-up of $E_W$ (0.07 to 1.5 $Wm^{-2}$) [Fig. 4 (b)] during phase II reached a maximum on 30 June and was followed by a decline. Correspondingly, an increase in the nocturnal maxima of the upward flux in $B_0$ (cooling) (1.6 to 2.4 × $10^{-7}$W $kg^{-1}$) [Fig. 4 (d)] was followed by a decrease after 30 June. The diurnal maxima of downward flux in $B_0$ (heating) (−4 to −1.3 × $10^{-7}$ W $kg^{-1}$)

TABLE 1

**Correlations between MLD and the vertical flux parameters of $B_0$, $U^3$ and $U_*^3$ at 0°, 60°E during Phases I and II of southwest monsoon in 1973 (Starred values of $r$ are significant at 95%)**

| Phase | Domain | No. of data pairs $n$ | Correlation coefficient ($r$) | | |
|---|---|---|---|---|---|
| | | | $B_0$ | $U^3$ | $U_*^3$ |
| I | (i) No. convection ($L > 0$) | 53 | 0.39* | 0.40* | 0.37* |
| | (ii) Convection ($L < 0$) | 131 | 0.31* | 0.29* | 0.24* |
| | Mixed | 184 | 0.54* | 0.34* | 0.31* |
| II | (i) No convection ($L > 0$) | 49 | 0.45* | 0.18 | 0.17 |
| | (ii) Convection ($L < 0$) | 117 | 0.24* | 0.16* | 0.14 |
| | Mixed | 166 | 0.17* | 0.08 | 0.07* |

progressively decreased after reaching the maximum on 26 June. Variability in MLD (−7 to −51 m) [Fig. 4 (f)] during the phase reflects a shoaling during 26-27 June, followed by a steady deepening. On daily mean values, barring the initial day, ML deepening by 20 m corresponded to a cooling by 1°C in 6 days (26 June to 2 July). However, dominances in ML responses were for momentum flux between 26 June and 30 June and for buoyancy flux before and after this period.

Analysis of variability of the Monin-Obukov Length ($L$) [Fig. 5 (b)] indicates that the convective mixing of ML ($L < 0$) became more active between 28 June and 2 July. Except at the beginning and end of the phase (25/26 June and 1/2 July) [Fig. 5 (d)] during which ML deepening was dominantly influenced by buoyant production ($D/L > 1$) and wind induced deepening ($D/L < 1$) was dominant during the phase.

Results on linear correlations examined between MLD, $B_0$, $U^3$ and $U_*^3$ in cases of diurnal convection, no convection and combination respectively for both phases are presented in Table 1. In general, relatively higher values of correlation coefficient ($r$) between MLD and $B_0$ suggest the dominance of buoyancy fluxes in the transfer of TKE for mixing in the upper layers during phase I. This observation agrees with the earlier studies on the atmospheric

TABLE 2

**Correlations between $Q_N$, $HC_{MLD}$, $HC_{50}$, $HC_{50\text{-}100}$ and $HC_{100\text{-}200}$ (Starred values of $r$ are significant at 95%)**

| Phase | No. of data pairs | Correlation coefficient ($r$) | | | |
|---|---|---|---|---|---|
| | | $HC_{MLD}$ | $HC_{50}$ | $HC_{50\text{-}100}$ | $HC_{100\text{-}200}$ |
| I | 184 | 0.54* | 0.04 | 0.07 | 0.04 |
| II | 166 | 0.18* | 0.05 | 0.08 | 0.11 |

boundary layer at the site during the period, also concluding on the predominance of buoyancy effects during May, compared to June when mechanical processes became significant (Ramanathan 1978). During the active regime of phase II, even the relatively higher correlations of $B_0$ with MLD decreased to insignificant values as a result of increasing lateral fluxes.

### 3.4. *Thermohaline and density fields*

During the pre-onset monsoonal transformations of phase I [Fig. 6 (a)], the progressive crowding and shoaling of the isotherms, especially between 50-150 m interval observed upto 31 May, coincided with the decrease in MLD in response to the decrease in wind stress momentum and increase in downward flux of $B_0$. The following spreading of isotherms upto 3 June was in response to the increase in wind stress and upward flux of $B_0$ at the surface. While variations in the thermocline gradients were between 0.15°C and 0.17°C $m^{-1}$, salinity variations [Fig. 6 (c)] were with weak vertical gradients [< 0.001 PSU $m^{-1}$]. The resultant density (sigma-T) [Fig. 6 (e)] changes closely followed the isotherm variability with a range in pycnocline gradient of 0.04-0.08 $m^{-1}$. Progressive changes in the temperature-salinity (T-S) characteristics (Fig. 7) observed during the phase suggests notable transformations in the upper 100 m. An overall reduction in the upper layer salinity resulted mainly due to the disappearance of the subsurface salinity maximum [> 35.4 PSU] after 1 June following the onset of SW monsoon. This may be due to the advection of relatively low salinity water brought into the monsoon drift by the intensifying recirculation of Somali Gyre, being fed by the low salinity south equatorial current water (SECW) [< 35.3 PSU] as investigated by Swallow *et al.* (1983).

During phase II, significant spreading of the isotherms [Fig. 6 (b)] resulted in the reduction of the thermocline gradients in the range of 0.10-0.12°C $m^{-1}$. Gradual increase in MLD and the isotherm

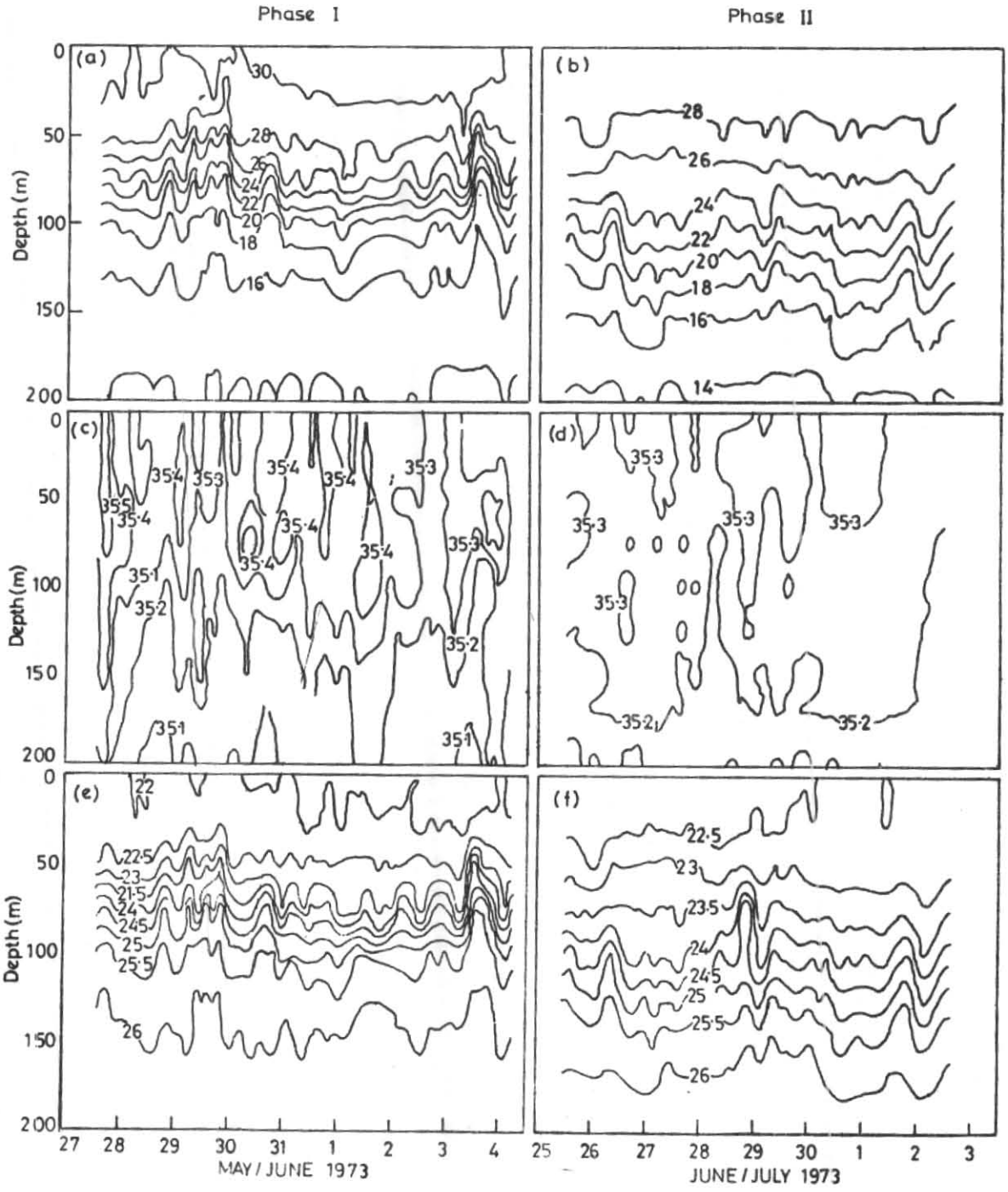


Figs. 6 (a-f). Time variation of temperature, salinity and density (Sigma-T) in the upper 200 m of the ocean during phases I and II

depths with time was in response to the increasing wind stress during the phase. Salinity field also [Fig. 6 (d)] showed appreciable reduction in the vertical gradient, compared to that of phase I. Spreading of isolines of sigma-T [Fig. 6 (f)] was in close agreement with the isotherm spreading as observed earlier (Gangadhara Rao *et al.* 1981), with pycnocline gradients ranging between 0.02-0.03 $m^{-1}$. The absence of the sub-surface salinity maximum is apparent from the nearly uniform vertical salinity distribution in the upper layers, as seen in the T-S plots for Phase II (Fig. 7).

### 3.5. *Variability of heat content*

Variations in the heat content of ML ($HC_{MLD}$) [Fig. 8 (a)] showed a decrease till 30 May and an increase thereafter as a result of the corresponding

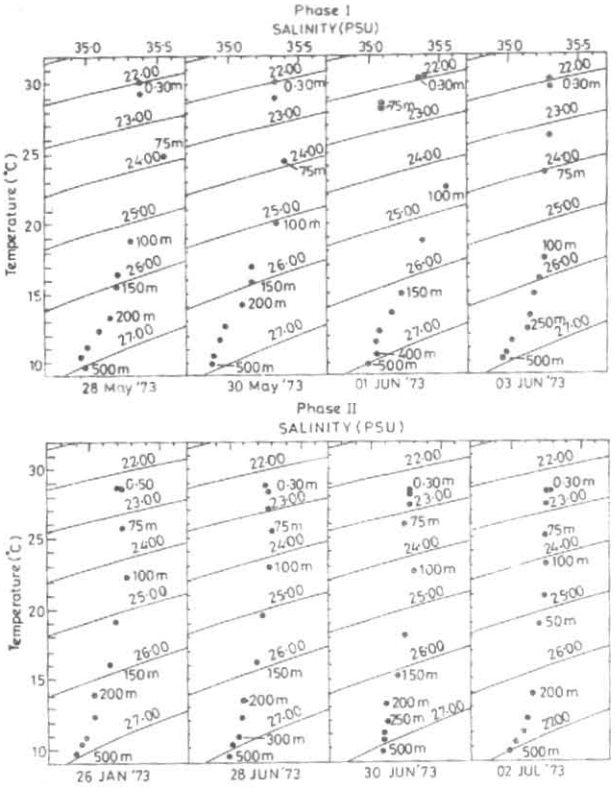


Fig. 7. Progressive T—S plots for phases I and II

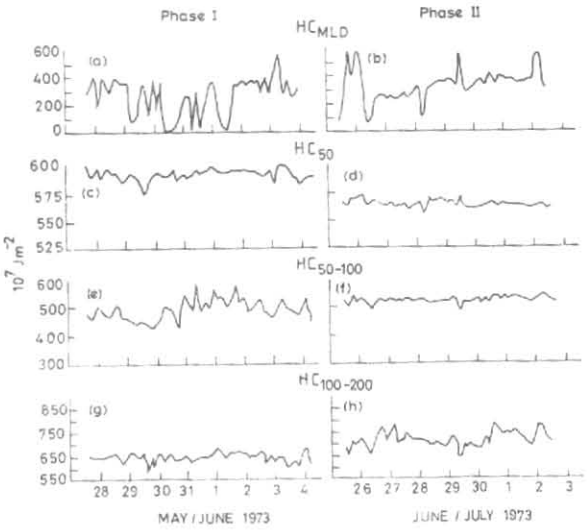


Figs. 8 (a-h). Time variation of heat content (a) and (b) within ML ($HC_{MLD}$), (c) and (d) 0-50 m ($HC_{50}$), (e) and (f) 50-100 ($HC_{50-100}$) and (g) and (h) 100-200 m ($HC_{100-200}$) during phases I and II

increase and decrease in MLD. The changes in heat content at 50 m ($HC_{50}$) [Fig. 8 (c)] were minimum with a nearly uniform progression, except for the decreasing events on 29 May and 4 June. After 30 May, a rise in heat content between 50 and 100 m ($HC_{50-100}$) [Fig. 8 (e)] possibly from a relatively warmer and low saline source like SECW, was evident, while the heat content between 100 and 200 m ($HC_{100-200}$) [Fig. 8 (g)] showed nearly constant progression during the phase.

Consequent to the deepening of ML, $HC_{MLD}$ increased progressively during phase II [Fig. 8 (b)], with episodic hikes on 25, 26, 28, 29 June and 2 July. $HC_{50}$ [Fig. 8 (d)] showed progressive decrease as a result of the cooling at the surface. However, heat content variability at the lower levels suggested an overall rise with gradual increase in the magnitude during the active regime as indicated by the progression of $HC_{50-100}$ and $HC_{100-200}$ [Figs. 8 (f & h)]. Linear correlations between $Q_N$, $HC_{MLD}$, $HC_{50}$, $HC_{100}$, $HC_{50-100}$ and $HC_{100-200}$ were analysed for phases I and II and presented in Table 2. Significant correlations existed only for $HC_{MLD}$ for which higher values in $r$ indicate greater dependence of $HC_{MLD}$ on $Q_N$ for phase I, while such dependence is greatly reduced as indicated by the low value of $r$ for phase II.

TABLE 3

**Initialising parameters for the mixed layer simulation**

| Parameter | Phase I | Phase II |
|---|---|---|
| MLD (m) | 32 | 17 |
| SST (°C) | 30.3 | 28.8 |
| Sea surface salinity (PSU) | 35.44 | 35.21 |
| Vertical temperature gradient just below MLD (°C m$^{-1}$) | 0.054 | 0.044 |
| Vertical salinity gradient just below MLD (PSU m$^{-1}$) | 0.0000 | 0.0045 |
| Extinction coefficient, $r$ (m$^{-1}$) | 0.2 | 0.2 |
| Mixing coefficient, m | 0.0009 | 0.0009 |

### 3.6. *Simulation of ML response*

One-dimensional simulation of the mixed layer progression during phases I and II was carried out under the assumption of negligible lateral advection following procedures of Denman (1973) and Miller (1976). Extinction coefficient ($r$) and the mixing coefficient of mechanical energy (m) were taken to be same for both phases. The initialising input parameters and the constants for the simulation model are presented in Table 3. Results of the simulations (Fig. 9) show that agreements between simulated and observed values of MLT were high for both phases (RMS departures : 0.18 and 0.15°C

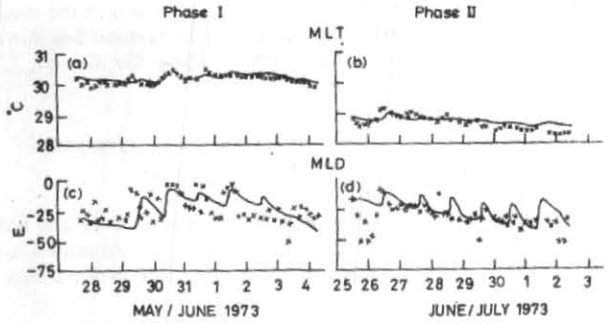


Figs. 9 (a-d). Time variation of observed (×××) and simulated (———) mixed layer temperature (MLT) and depth (MLD) during phases I and II

respectively). Corresponding agreements in MLD indicated to be reasonable (RMS departures : 12.4 and 11.5 m respectively) as the simulation model accounts for no wave like motions.

## 4. Summary and conclusions

Analysis of data at 0°N. 60°E during the *in situ* pre-onset. onset and active regimes of SW monsoon in May/June/July 1973 indicated the following.

The pre-onset slackening and onset strengthening of the wind field was associated with the corresponding increase and decrease in $Q_N$ before and after 1 June 1973. Resulting upper layer responses manifested in the pre-onset shoaling/warming of ML (by 12 m/0.5°C in 4 days from 27 to 30 May) under slackening wind dominance after 28/29 May and onset deepening/cooling of ML (at the same rate) under increased dominance of buoyant production of TKE from 31 May to 4 June.

Corresponding pre-onset crowding/shoaling and onset deepening/spreading of isopleths in 50-150 m interval resulted in the respective increase and decrease in gradients. Increased warm and low saline advective flux, possibly of SECW. resulted in the disappearance of sub-surface salinity maximum and increase in heat content in the 50-100 m interval after the monsoonal onset by 1 June.

Active regime of SW monsoon (as observed during 25 June-2 July) was characterised by the gradual strengthening (upto 29 June) and following slackening of the wind stress, invoking continuous decrease in SST/AT/RH and increase in cloud cover after 1 June. During active regime in June/July, magnitude and diurnal range in $Q_N$ decreased mainly due to the increase in cloudiness and decrease in $Q_e$ especially after 29 June. ML deepening/cooling (by 20 m/1°C in 6 days from 26 June to 2 July) was affected by dominance of wind production (26 June to 1 July) and convective production (25/26 June and 2 July) of TKE.

General reduction of the thermohaline/density gradients in 50-150 m interval and the continued absence of the sub-surface salinity maximum were apparent in the active regime.

Correlations between MLD/HC of ML and $B_0$/$Q_M$ were more in the pre-onset and onset regimes, while they became increasingly insignificant due to the possible increase in lateral fluxes. One dimensional simulation of the progression of MLT and MLD resulted in reasonal agreements with that observed for both phases (RMS differences : 0.18°C and 12.4 m for phase I and 0.15°C and 11.5 m for phase II).

*Acknowledgements*

Our sincere thanks are due to the ISMEX Management Committee and India Meteorological Department for the data supplied. We are grateful to the Director, Naval Physical and Oceanograpahic Laboratory, Cochin, India for encouraging and supporting the work.

### References

Atwater, M. A. and Ball, J. T., 1981, "A surface solar radiation model for cloudy atmosphere", *Mon. Wea. Rev.*, **109**, 880-888.

Friehi, C. A. and Schmitt, K. F., 1976, "Parameterisation of air-sea interface fluxes of sensible heat and moisture by aerodynamic bulk formulas", *J. Phys. Oceanogr.*, **6**, 801-809.

Gangadhara Rao, L. V., Ramesh Babu, V. and Varadachari, V. V. R., 1981, "Structure of currents and hydrographic conditions in the western equatorial Indian Ocean during the summer monsoon". In : *Monsoon Dynamics*, Eds. Lighthill, J. and Pearce, R. P., Cambridge University Press, London, 453-463.

Godwin, E. M. and Kemp, J. F., 1979. *Marine Statistics*, Stanford Maritime Ltd., London, 336 pp.

Joseph, M. G., Hareesh Kumar, P. V. and Basil Mathew, 1990, "Short term pre-onset southwest monsoonal transformations in upper western equatorial Indian Ocean", *Indian J. Ma. Sci.*, **19**, 251-256.

Joseph, M. G., Hareesh Kumar, P. V. and Joseph, M. X., 1992, "Deep and shallow water characteristics of mixed layer

response to momentum and buoyancy fluxes off Bombay, west coast of India, during winter", *Cont. Shelf Res.*, **12**, 661-673.

Kato, H. and Phillips, O. M., 1969. "On the penetration of turbulent layer into stratified fluid", *J. Fluid Mechanics*, **37**, 643-655.

Lumb, F. E., 1964, "Influence of cloud on hourly amount of solar radiation", *Quart. J. Roy. Met. Soc.*, **90**, 43-56.

Mc Phaden, M. J., 1982, "Variability in the central equatorial Indian Ocean, II, Oceanic heat and turbulent energy balances", *J. Mar. Res.*, **40**, 403-419.

Molinari, R. L., Swallow, J. C. and Festa, J. F., 1986, "Evolution of the near-surface thermal structure in the western Indian Ocean during FGGE, 1979", *J. Mar. Res.*, **44**, 739-762.

Pant, M. C., 1976, "Structure of the southwest monsoon near the equator during MONEX-1973", *Indian J. Met., Hydrol. Geophys.*, **27**, 1-8.

Payne, R. E., 1972, "Albedo of the sea surface", *J. Atmos. Sci.*, **29**, 959-970.

Ramanathan, Y., 1978, "Atmospheric boundary layer over Arabian Sea", *Indian J. Met. Hydrol. Geophys.*, **29**, 643-654.

Rao, R. R., 1986, "Cooling and deepening of the mixed layer in the central Arabian Sea during MONSOON-77 : Observations and simulations", *Deep-Sea Res.*, **33**, 1413-1424.

Rao, R. R., Molinari, R. L. and Festa, J. F., 1989, "Evolution of the climatological near-surface thermal structure of the tropical Indian Ocean, 1. Description of mean monthly mixed layer depth, and sea surface temperature, surface current, and surface meteorological fields", *J. Geophys. Res.*, **94**, 10801-10815.

Rao, R. R. and Basil Mathew, 1990. "A case study of the mixed layer variability in the south central Arabian Sea during the onset phase of MONEX-79", *Deep-Sea Res.*, **37**, 227-243.

Reed, R. K., 1977, "On estimating insolation over the ocean", *J. Phys. Oceanogr.*, **7**, 482-485.

Sanil Kumar, K. V., Madhusoodanan, P., Joseph, M. G. and Basil Mathew, 1991, "Mixed layer variability in east central Arabian Sea during premonsoon season of 1979", *Indian J. Mar. Sci.*, **20**, 239-243.

Shay, T. J. and Gregg, M. C., 1986, "Convectively driven turbulent mixing in the upper ocean", *J. Phys. Oceanogr.*, **16**, 1777-1798.

Shetye, S. R., 1986, "A model study of the seasonal cycle of the Arabian Sea surface temperature", *J. Mar. Res.*, **44**, 521-542.

Swallow, J. C., Molinari, R. L., Bruce, J. G., Brown, O. B. and Evans, R. H., 1983, "Development of near-surface flow pattern and water mass distribution in the Somali basin in response to the Southwest Monsoon of 1979", *J. Phys. Oceanogr.*, **13**, 1398-1415.

Turner, J. S., 1969, "A note on wind mixing at the seasonal thermocline", *Deep-Sea Res.*, **19**, 297-300.

Wyrtki, K., 1966, "Seasonal variation of heat exchange and surface temperature in the north Pacific Ocean", Hawaii Institute of Geophysics Report HIG. 66-3, University of Hawaii, Honolulu, 8 pp.